

STELLAR WIND PALEONTOLOGY. II. FAINT HALOS AND HISTORICAL MASS EJECTION
IN PLANETARY NEBULAEBRUCE BALICK,¹ GUILLERMO GONZALEZ,¹ AND ADAM FRANK¹

Astronomy Department, University of Washington

AND

GEORGE JACOBY²Kitt Peak National Observatory, National Optical Astronomy Observatories³

Received 1991 October 4; accepted 1991 December 27

ABSTRACT

The large, faint, generally circular, and limb-brightened nebular structures (called “halos”) surrounding some planetary nebulae (PN) are explored using deep CCD images of NGC 40, 650–1, 1535, 2392, 6210, 6543, 6720, 6803, 6804, 6826, 6853, 6891, 6894, 7009, 7662, IC 1454, 3568, 4593, Abell 1, 2, 3, and BD +30°3639. New halos have been discovered in a few objects (IC 1454, 4593, and possibly NGC 40, 6210, and 6803), and known halos have been mapped in detail in several PN (e.g., NGC 6543, 6720, 6826, 6853 and 7662). Surprisingly, our deep search does not reveal similar large and faint halos in NGC 1535, 2392, 6894, 7009, and IC 3568—PN whose inner regions are morphologically similar to others with easily observable halos.

Halos are believed to represent early episodes of mass ejection from the central star. The detected halos are all limb-brightened, characterized by radii of ≈ 0.3 – 0.5 pc, and are more circular than the PN which they surround. All of the newly detected halos as well as those previously identified have the emission measure distributions expected after $\approx 10^4$ yr if hydrodynamic effects control the evolution of the mass distribution of ejecta from the nucleus, as described by Frank, Balick, & Riley in 1990.

Subject headings: planetary nebulae: general — stars: mass loss — ISM: structure

1. INTRODUCTION

Surrounding the bright cores of many planetary nebulae are “envelopes” extending out to radii of 0.5 pc in exceptional cases (Chu, Jacoby, & Arendt 1987, hereafter CJA; Jewitt, Danielson, & Kupferman 1986; Kaler 1974; and Millikan 1974). Envelopes are a general term for outer structures which include shells, halos, and an assortment of other features. This is the second in a series of papers that exploits the structure of common morphological features to explore the history of mass loss from the nuclei of PN.

In this paper we focus on the outermost symmetric nebulosities of PN called “semi-detached shells” by CJA and “halos” in this paper. Owing to the confusion of nomenclature in the literature, we wish to be very precise in our operational definitions of structural components. As used here and in Paper I,

1. “Cores” are defined to be compact (radii $r_h \leq 0.03$ pc), thin, and very bright circular or elliptical structures concentric with the nuclei of most nonbipolar PN,

2. “Shells” are larger ($r_h \approx 0.1$ pc), sharply bounded, often linearly decreasing plateaus of emission surrounding most cores (see Paper I for a full phenomenological description), and

3. “Halos” are low-surface-brightness, round, and *always limb-brightened* structures that can sometimes appear to be detached from shells in short-exposure images. Typical radii are 0.3 pc with large variations from nebula to nebula.

¹ Postal address: Astronomy Department FM-20, University of Washington, Seattle, WA 98195.

² Postal address: Kitt Peak National Observatory (KPNO), P.O. Box 26732, Tucson, AZ 85726-6732.

³ Operated by the Association of Universities for Research in Astronomy, Inc., under cooperative agreement with the National Science Foundation.

Additionally, some PN envelopes contain faint but patchy or irregular outer structures, which we designate in general as “outer flocculi.” When the distribution of flocculi has a nearly circular distribution with a sharp outer or “leading” edge, we consider the flocculi to be part of a halo, as in the well-known case of NGC 6543. Examples of flocculi appear in the figures below.

The geometric relationships between cores, shells, and halos has been discussed in several papers, such as Balick (1987, hereafter B87), CJA, and Paper I. The “standard model” is one in which a relatively small, bright core is surrounded by a fainter smooth shell around which is an even fainter, sometimes marginally detectable halo. However, not all of these morphological components are found in all round or elliptical PN. For example, many PN such as NGC 1535, 2392, and IC 3568 have bright cores and shells but no detectable halos. Other PN are opposite: they are virtually all halo with no core or shell (e.g., Abell 30 and 39).

All PN with shells have cores, though not all cores are associated with shells, e.g., BD +30°3639. (This may be because some cores are opaque to ionizing radiation from the nucleus, so any outer structures are not visible in emission from ionized species.) Halos are difficult to detect, and statistics on their correlation with other features are incomplete. To date, all halos are associated with round or elliptical PN.

The putative origin of cores, shells, and halos is worthy of a brief review. Paper I and Tuchman & Barkat (1980, and references within) called attention to the significance of PN shells and halos surrounding the cores of PN as possible fossil evidence of historical ejections of stellar material which were expelled percussively within the past few thousand years.

As a star evolves along the AGB it deposits mass at low

velocity (10 km s^{-1}), a “slow wind”, into the space which surrounds it. This may happen repeatedly forming several pulses of slow winds. After a few thousand years, as the nucleus becomes a source of ionizing radiation, a fast wind (10^3 km s^{-1}) begins. In the process a very hot, tenuous, high-pressure, optically invisible bubble forms around the star which expands and rams into the older slow wind from the inside. Cores are believed to be material at the inner edge of the last pulse of slow wind which is snowplowed by the expanding hot bubble. They are not discussed further here (see Marten & Schönberner 1992 for a discussion of the evolution of cores). In Paper I we argued that shells are relatively recent slow wind pulses expanding into the ISM which, as yet, are unaware of the onset of the fast wind. As they expand their surface brightness drops and they tend to become limb-brightened. Halos are relatively old ($> 10^4 \text{ yr}$) and highly evolved shells.

One-dimensional time dependent hydrodynamical code was used in Paper I to reproduce the radial intensity distributions of PN shells and halos. The goal was to untangle the effects of hydrodynamical evolution of the mass distribution from the history of ejection and, thereby, to place some limits and constraints on the duration, velocity, and mass-loss rates of the slow wind ejection process. The model calculations imply that PN shells and halos have masses of $\sim 0.25 M_{\odot}$, and that the pulse of ejected mass is characterized by a fast rise and somewhat slower decline spanning $\sim 2000 \text{ yr}$. In Paper I the discussions focussed on shells because the quality of observations of halos was relatively poor.

We have attempted to provide better observations of halos for which good quantitative data are scarce. In addition we have searched for faint halos around other PN in which halos have not been detected. Specifically, since NGC 2438, 6720, 6751, 6826, 6853, 6891, 7662, and IC 1295 (CJA and references within) all have been known to have faint round halos, one might expect to find halos in many other PN with similar morphologies such as NGC 1535, 2392, 2610, 3242, 6894, 7354, IC 289, and 3568. We have observed some of the latter set of nebulae. In addition other generally bright PN were observed simply because they were accessible, and not because we had any reason to suspect the existence of a halo.

Hereafter north, east, south, and west are abbreviated N, E, S, and W, respectively. The emission lines $\text{H}\alpha$ $\lambda 6563$, $[\text{N II}]$ $\lambda 6583$, and $[\text{O III}]$ $\lambda 5007$ are henceforth designated $\text{H}\alpha$, $[\text{N II}]$, and $[\text{O III}]$, respectively. All images are shown as the logarithm of the intensity in order to decrease the contrast between core and a faint halo or the background noise level. Readers should be aware of the resulting highly nonlinear transformation and the exaggeration of faint features and noise.

2. OBSERVATIONS

The data presented here were obtained using the 4 m Mayall telescope at the Kitt Peak National Observatory (KPNO) with the prime focus CCD and the 0.8 m telescope of the Manastash Ridge Observatory (MRO) with the Cassegrain CCD camera. Cirrus cover was present for some of the observations and may have affected the transparency by about 20%. The seeing was generally better than $2''$.

The 4 m observations were conducted 1990 July 24–25 and August 10–11 (during summer engineering tests) using a Tektronix 1024×1024 CCD with 75 \AA (FWHM) narrowband filters centered at $\text{H}\alpha$ and $[\text{O III}]$. The focal ratio is $f/2.7$, so the resulting pixels scale is $0''.48$. The seeing was about $1''$, so the data were subsequently rebinned to a resolution of $0''.96$ in

order to improve the signal-to-noise ratio without degrading the image quality significantly. The CCD is ideal for studying halos owing to its low readout noise ($3e^-$), large full-well capacity ($200,000e^-$), and high quantum efficiency ($> 80\%$). No observations of standard stars were attempted owing to variable atmospheric transparency. Assuming net telescope throughput of 40%, 1 detected CCD electron per second per pixel corresponds to a surface brightness of $1.5 \times 10^{-15} \text{ ergs s}^{-1} \text{ cm}^{-2} \text{ arcsec}^{-2}$. In order to preserve details of the very bright cores and faint halos multiple short exposures were taken and then added during the data calibrations. Even so, the nebular cores are sometimes badly saturated. Nebula/total exposure time (s)/filter combinations of the KPNO images are the following: NGC 40/300/ $\text{H}\alpha$; NGC 650–1/600/ $[\text{O III}]$; NGC 6210/480/ $\text{H}\alpha$; NGC 6543/600/ $\text{H}\alpha$; NGC 6720/200/ $\text{H}\alpha$; NGC 6803/360/ $\text{H}\alpha$; NGC 6804/600/ $\text{H}\alpha$; NGC 6826/400/ $\text{H}\alpha$; NGC 7009/60/ $\text{H}\alpha$; NGC 7662/6600/ $\text{H}\alpha$; IC 1454/900/ $[\text{O III}]$; IC 3568/17/ $\text{H}\alpha$; IC 4593/900/ $\text{H}\alpha$; Abell 1/600/ $\text{H}\alpha$; Abell 2/600/ $\text{H}\alpha$; Abell 2/600/ $[\text{O III}]$; Abell 3/1200/ $[\text{O III}]$; and BD $+30^{\circ}3639/240/\text{H}\alpha$. Halos characteristically produce about 0.1 to 10 detected electrons per minute in each CCD pixel.

Data were obtained on the 0.8 m telescope in 1990 August and September. The detector is a Ford Aerospace 1024×1024 CCD. Reimaging optics in the camera produce an $f/6.75$ beam, or $0''.7/\text{pixel}$, and a field of view of $12'$. On-chip (2×2) binning effectively reduced the f ratio by half and doubled the projected pixel size. The DQE of the chip is 50% between 5000 and 7000 \AA . Two 20 \AA -wide filters centered at 6563 \AA (hereafter the “ $\text{H}\alpha$ filter”) and 6585 \AA (the “ $[\text{N II}]$ filter”) were used with the MRO CCD. The transmission of these filters at wavelengths of emission lines is shown in Table 1. Clearly, there is some leakage in the filters to strong nearby emission lines. Observed $[\text{N II}]$ $\lambda 6548$: $[\text{N II}]$ $\lambda 6583$: $\text{H}\alpha$ emission line ratios are typically 0.03:0.1:1, so our $\text{H}\alpha$ images may contain a $\approx 5\%$ contribution from the $[\text{N II}]$ lines. However, as much as half of the emission through the $[\text{N II}]$ filter can be $\text{H}\alpha$ contamination! For these reasons we do not attempt to measure absolute values of the intensity ratio of $[\text{N II}]$ $\lambda 6548 + \lambda 6583$ to $\text{H}\alpha$ or to correct for atmospheric attenuation.

Nebula/total exposure time (s)/filter combinations for the MRO observations are the following: NGC 40/600/ $\text{H}\alpha$; NGC 40/600/ $[\text{N II}]$; NGC 1535/500/ $\text{H}\alpha$; NGC 2392/1200/ $\text{H}\alpha$; NGC 2392/1200/ $[\text{N II}]$; NGC 6543/600/ $\text{H}\alpha$; NGC 6543/600/ $[\text{N II}]$; NGC 6720/2000/ $\text{H}\alpha$; NGC 6720/1000/ $[\text{N II}]$; NGC 6826/600/ $\text{H}\alpha$; NGC 6826/600/ $[\text{N II}]$; NGC 6853/4000/ $\text{H}\alpha$; NGC 6894/1000/ $\text{H}\alpha$; NGC 6894/1000/ $[\text{N II}]$; NGC 7009/1200/ $\text{H}\alpha$; NGC 7662/1700/ $\text{H}\alpha$; and NGC 7662/200/ $[\text{N II}]$. Occasional heavy cirrus prevented a calibration of surface brightnesses.

The detection of faint halos is limited by internal reflections, scattering, and imperfections in the optics as well as by the signal-to-noise ratio. The problems are of three general types: internal reflections in reduction optics and the camera appearing as toroids; diffraction and imperfections in the telescope optics appearing as faint spikes, collars, and rings around all bright objects; and miscellaneous reflections seen as daggers or

TABLE 1
MEASURED FILTER TRANSMISSIONS

Emission Line	$[\text{N II}]$ $\lambda 6548$	$\text{H}\alpha$	$[\text{N II}]$ $\lambda 6583$
$\text{H}\alpha$ filter	50.1%	68.3%	4.0%
$[\text{N II}]$ filter	< 1	8.5	61.48

arcs of light in random places on the CCD. Only the second type of problem was found in the 4 m images. The magnitude of the detected light at $\geq 10''$ or more from a bright object is $\leq 10^{-4}$ of the peak brightness.

However, all types of problems were seen in frames obtained at MRO. The brightest of these are internal reflections which can be easily identified owing to their highly characteristic donut and dagger-like shapes. The donut pattern is fiendishly similar to the faint, round halos that we were hoping to detect. Consequently, when faint halos were seen in any frame the telescope's pointing position was dithered by a quarter of the field of view. The dithering causes reflections to move with respect to the PN and any associated halo. In this manner any interfering internal reflections were moved to the edges of the CCD image. This procedure could not be implemented for NGC 6853 which overfills the field of the CCD. Internal reflections in that PN are not noticeable in the final mosaic image although they may be present at low levels.

With a few exceptions, the newly found halos are 10^4 times lower in surface brightness than the corresponding PN cores. Aside from the problems above, the core can badly saturate the CCD and cause tails and other problems to appear after readout. Hence for the second run at MRO one of us (G. G.) prepared a mask of an aluminized spot to be placed near the telescope's focus in front of the reducing optics to block out the light from a $50''$ diameter portion of the sky. With this "coronagraphic spot" mask many of the program objects were observed repeatedly for about 2000 s. No additional halos were uncovered, and the halos observed in the first run were verified.

KPNO and MRO data were calibrated using standard and very straightforward procedures.

3. RESULTS

The results for the present sample of PN are presented individually by PN.

NGC 40 (PK 120 + 9° I).—Outer flocculi to the NE of this well-known PN have been noted in NGC 40 previously (Louise 1981; B87; CJA). The KPNO image (Fig. 1) shows an additional network of faint flocculi extending to the S and W. However, the morphologies of the flocculi divide into two groups: the brighter flocculi to the N and E (0.1%–0.5% of the brightness of the core) are very knotty. In contrast the fainter flocculi to the S (0.03% of the core brightness) appear to be smooth filaments. It is possible that the two groups of flocculi have different origins or evolutions.

In many ways the morphologies of the outer flocculi of NGC 40 are the most complex of the PNs discussed in this paper. The large-scale brightness distribution of the flocculi to the N and E is roughly circular and limb brightened, suggesting that this gas was expelled or shaped by winds from the nucleus as in the halo of NGC 6543. The fainter filaments to the S and W have no particular symmetry with respect to the PN, and might be ambient ISM ionized by UV photons escaping from the core of NGC 40. Whether NGC 40 has a wind-blown halo is problematical. However, the comet-like tails on the knots of the N and E flocculi leave the impression that winds from the core have been active. Similar comet tails are seen in NGC 6543 and 6826.

A short digression on other structures found close to the bright core is in order. First, note a linear feature protruding S of the core in Figure 1. A fainter counterpart from the N end of the core connects to the W end of the NE flocculus. Such jets are unusual in PN, but not unprecedented; similar features

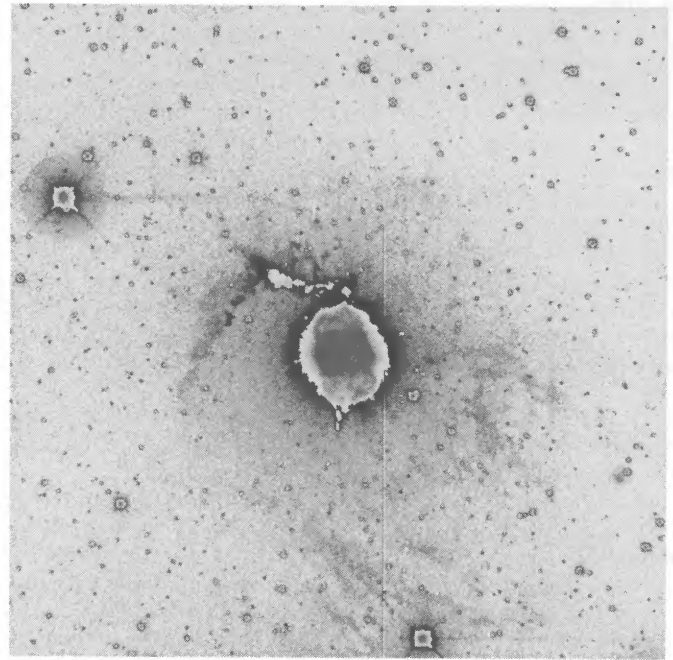


FIG. 1.—CCD image of NGC 40 in the indicated filter taken with the 4 m Mayall telescope at KPNO. The grayness is proportional to the logarithm of the intensity in order to exaggerate the faint features. Each pixel has been convolved to $0''.96$ on the sky. The field of view is 495×500 pixels ($0''.96$ pixel $^{-1}$). N is at the top and E is to the left.

were found in NGC 6543 and 7354 by B87. Also note a very smooth shell of radius $\approx 2'$ which surrounds the core. The shell is also seen in our MRO images and observed by B87. The shell is not unlike the scattered light which surrounds bright field stars in Figure 1 (although substantially larger in radius) so its reality is suspicious.

NGC 650-1 (PK 130-10° I).—This is an outstanding example of an object for which a short exposure tells a very different story from a long one (Fig. 2). Note how the position angle of the isophotal major axis changes by 90° from bright to faint structure. The same pattern is found for NGC 6853 (see below) and most bipolar nebulae. The inner section appears nearly rectangular in outline. The faint lobes are $284''$ in extent. Note the extremely sharp edges of the lobes. Since these are not ionization fronts (B87), the edges are probably the result of confinement by an invisible and presumably low-density medium.

No halo—i.e., a round, faint, large, limb-brightened structure—surrounds this bipolar nebula. Interestingly, no halo has been detected in any bipolar PN perhaps suggesting (1) that mass loss is collimated throughout the lifetime of ejection or (2) an opaque disk shadows ionizing radiation from the portions of a putative halo lying outside the disk.

NGC 1535 (PK 206-40° I).—The morphologies of the cores and shells of NGC 6826, 6891, and 7662, all PN which show faint outer halos, are strikingly similar to NGC 1535 (e.g., B87). Since the core of NGC 1535 is very bright we considered the PN to be a prime candidate for uncovering a faint outer halo. A 500 s exposure was made through the $H\alpha$ filter at MRO. No halo was detected to the average noise level of approximately

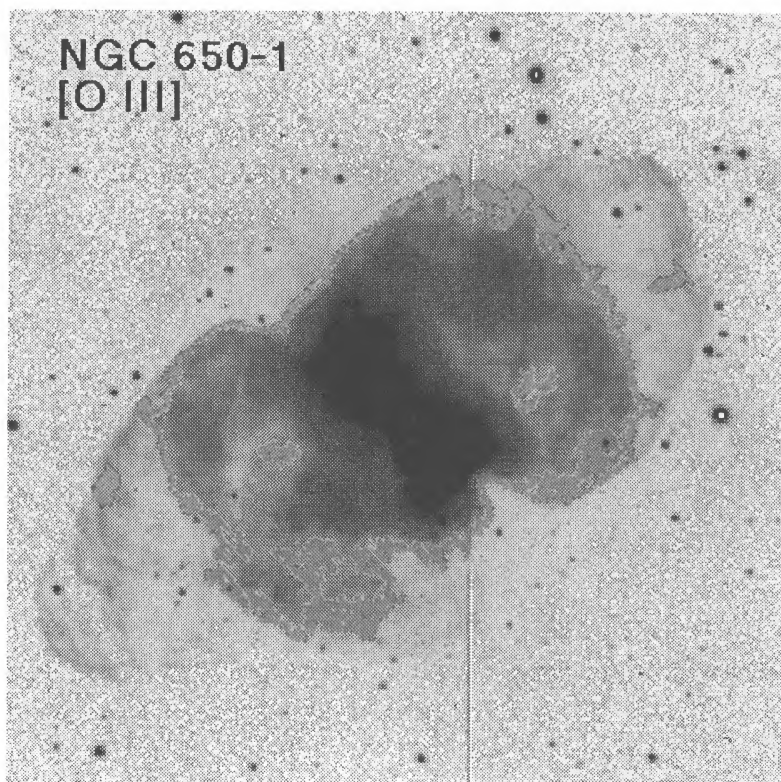


FIG. 2.—NGC 650—1. See also the caption of Fig. 1. The field of view is 300 pixels.

10^4 times fainter than the bright core. Longer exposures would not have helped to discover a faint halo since scattered light of the PN in the telescope optics dominates the image background outside the nebular image.

NGC 2392 (PK 197+17°1; the “Eskimo”).—Like NGC 1535, the Eskimo nebula shares many of the same morphological characteristics of other PN with halos. Also like NGC 1535, no halo was detected.

Observations were made at MRO through both the $H\alpha$ and $[N II]$ filters for 600 s. A 2000 s exposure was made during the second run using the $H\alpha$ filter and a coronagraphic spot to block direct light from the core and shell. Although light was detected from outside the shell, its distribution resembles that of scattered light from bright stars similarly observed. No halo is detected. The surface brightness limit for the halo is approximately a factor of 20,000 fainter than the peak nebular surface brightness.

NGC 6210 (PK 43+37°1).—The KPNO image (Fig. 3) shows a faint but definite shell (i.e., no limb brightening) whose brightness ends abruptly at a radius of $30''$. The surface brightness of the shell is more than 2000 times fainter than the core. The very knotty core is heavily overexposed (see B87 for images of the core). Extending from the E and W edges of the core through the shell are two pairs of peculiar spoke- or armlike features. Outside the shell is an arclike segment (marked by arrows in Fig. 3) that could be associated with an exceedingly faint halo. Deeper observations are needed to confirm the reality of the arc.

NGC 6210 was not observed at MRO owing to poor spring weather.

NGC 6543 (PK 96+29°1).—The patchy envelope of NGC 6543 was discovered by Millikan (1974). Comet-shaped flocculi

dominate the structure of the halo (Fig. 4). The sharp round outer boundary of the distribution of flocculi argues for the existence of a true halo of ejected stellar material. The characteristic surface brightness of the patches is about 10^4 times fainter than the peak nebular surface brightness. The physical

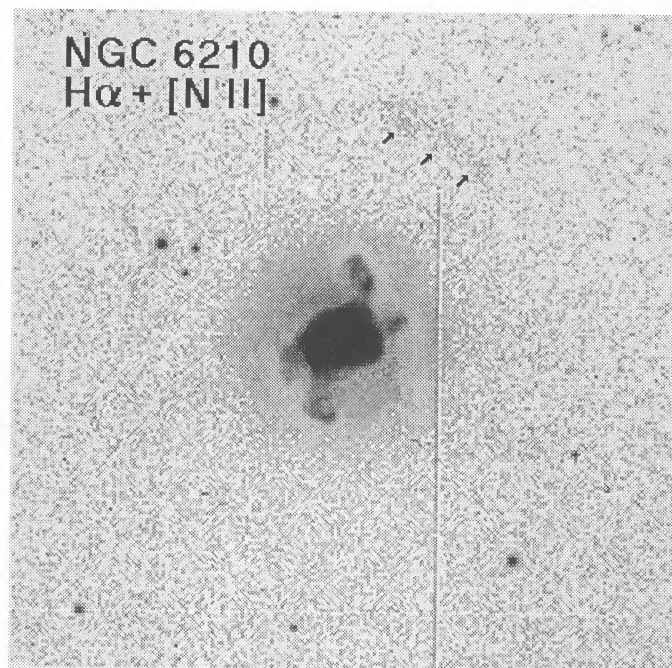


FIG. 3.—NGC 6210. See also the caption of Fig. 1. The field of view is 200 pixels.

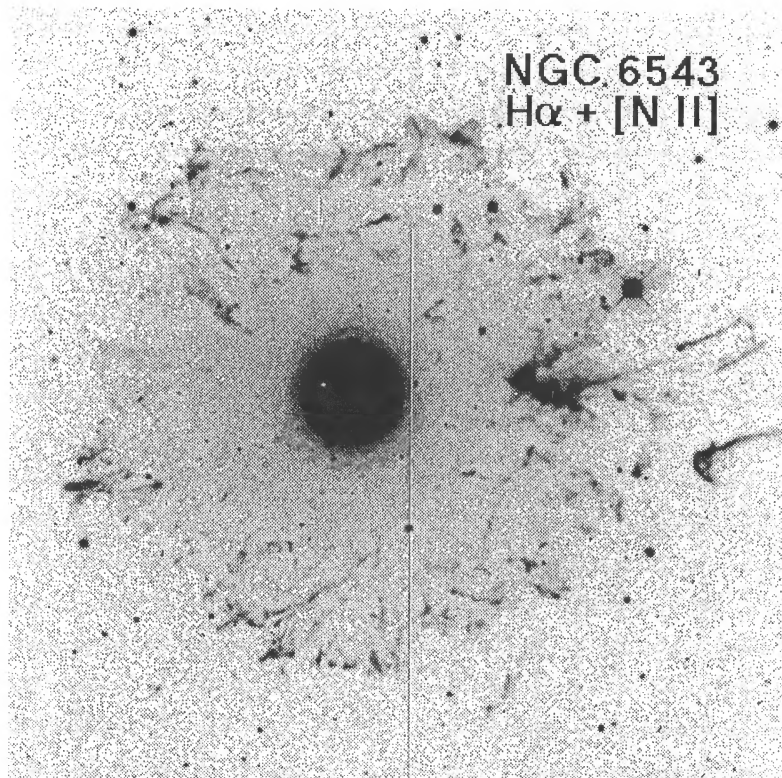


FIG. 4.—NGC 6543. See also the caption of Fig. 1. The field of view is 400 pixels.

and chemical properties of the flocculi have been discussed by Middlemass et al. (1991) and Meaburn et al. (1992) who suggest that they are shock excited. This, and the cometary morphologies of the flocculi can both result from a fast stellar wind which permeates the halo and produces bow shocks. See Dyson & Hartquist (1992) for a detailed discussion.

The radial distribution of intensity drops off much more smoothly than other halos. Its average radius is $170''$. However, the cometary nebulae dominate the fine-scale structure of the halo. One might conjecture that the halo of this object initially evolved as a smooth distribution of material, much like other halos. Subsequently, strong winds from the nucleus and resulting instabilities result in the formation of cometary flocculi. The references above explore this point in considerable detail.

NGC 6720 (PK 63+13°1; the “Ring Nebula”).—The appearance of a ragged halo surrounding the famous “Ring” (or core) has been noted by B87, Moreno & López (1987), and CJA, among others. The CCD image by CJA is the best of these exposures. CJA estimate that the angular diameter of this halo is $162'' \times 147''$. We find a average angular radius of $90''$ to the sharp intensity dropoff of inner halo and $115''$ for the outer one. Within this region are many looplike flocculi which are typically 0.5% of the core surface brightness.

The KPNO image obtained through the $H\alpha + [N II]$ filter in $\approx 1''$ seeing is shown in Figure 5. An outer and perfectly circular halo of radius $\approx 135''$ surrounds the inner halo seen by CJA. The surface brightness of the inner halo is about 1000 times less than the peak nebular brightness. The MRO images (which go even deeper but were obtained under conditions of poorer seeing) verify all of the features seen in the KPNO images. (No additional features are seen.)

The outer halo is about 5 times fainter than its inner counterpart. Images through very narrow $H\alpha$ and $[N II]$ filters by B87, though not long exposures, show clearly that *both* lines are emitted in the innermost of the two halos. MRO images through the $H\alpha$ and $[N II]$ filters confirm this. The image ratios are consistent with no change in this ratio averaged over the core, on the one hand, and the halo on the other. Careful spectroscopy of the halos is needed to see if any radial CNO abundance gradients might exist.

Figure 5 shows that the inner of the two halos consists of a series of large and small limb-brightened loops or petals, some smaller and/or more prominent than others. Along the loops the surface brightness oscillates regularly. These “pleats” of brightness with characteristic separations of 2–3” suggest that some type of collective instability is occurring. This, and the strong limb-brightening of the loops, argue for some sort of hydrodynamically induced process being responsible. Instabilities at the edges of cores have been discussed and reviewed by Breitschwerdt & Kahn (1990). A single long-slit spectrum by Chu & Jacoby (1989) shows that the $[N II]$ lines in these loops are split by 36 km s^{-1} .

The discovery of two limb-brightened halos in this nebula is unprecedented. Since halos are generally believed to be the remnants of former episodes of mass ejection, the core and two halos of NGC 6720 are the result of three pulses of mass ejection from the nucleus.

The distribution of molecular hydrogen has been mapped in NGC 6720 by Greenhouse, Hayward & Thronson (1988). Images in the $S(0) v = 1-0$ line of H_2 appear to be virtually the same as B87’s short exposures in the lines of $[N II]$ and $[O I] \lambda 6300$. The H_2 and these low ionization optical lines are seemingly coincident. All lines arise at the outer edge of the core or

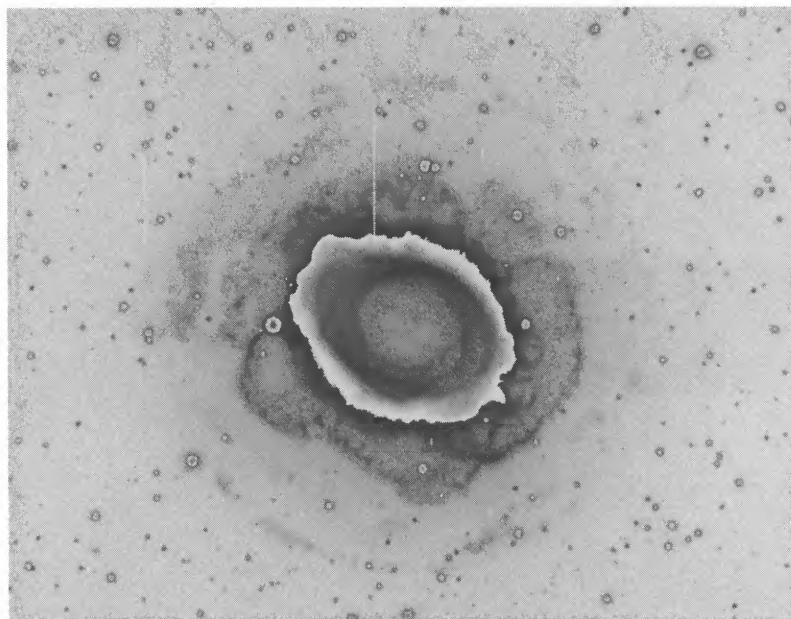


FIG. 5.—NGC 6720. See also the caption of Fig. 1. The field of view is 297×382 pixels.

“ring” from which the nebula derives its name. It is tempting to conclude that all of these lines arise in an ionization front (IF). We emphasize, however, that the two halos are seen in projection *outside* of the bright H_2 emission. This unexpected geometry is discussed further in the next section.

NGC 6803 (PK 46–4° I).—The core of this small PN is heavily saturated in the KPNO image (Fig. 6). An extremely faint halo of radius $\approx 30''$ is seen which is more than 3000 times fainter than the core. It could be an artifact of the optics of the telescope; however, deep images of bright stars do not show a similar feature with the same radius. The object was not observed at MRO.

NGC 6804 (PK 45–4° I).—The core of the nebula appears much like a pair of lips around which a smooth but partial shell is found (Fig. 7). The position angle major axis of the core is about 135° . There is a suggestion of limb brightening at the edge of the shell similar to that seen by B87 in the shells of NGC 3242, 7354, and 7662. The overall morphology is common to NGC 2610, 7354, and IC 289 (B87).

Very faint smooth flocculi, found first by CJA, lie along an axis which is perpendicular to the major axis of the core. We do not consider these to comprise a halo owing to the absence of circular symmetry and limb brightening. However, deeper integrations could show the flocculi to be part of a halo.

NGC 6826 (PK 82+11° I).—The strikingly circular halo of NGC 6826 is one of the brightest and best studied (e.g., Plait & Soker 1990; Paper I). Our deep KPNO image obtained in excellent seeing is shown in Figure 8. The halo has a mottled, filamentary appearance and a radius of $68''$ to the steep intensity gradient at the outer edge of the halo. The nebular core is about 2000 times brighter than the halo. MRO images suggest that the $[N II]/H\alpha$ ratio is constant throughout the halo; however, the leakage of the very strong $H\alpha$ line into the $[N II]$

filter passband limits the validity of this assertion. Spectroscopic observations of the halo of NGC 6826 are summarized and discussed by Middlemass et al. (1991). Chu & Jacoby (1989) report an expansion velocity close to the sound speed (10 km s^{-1}).

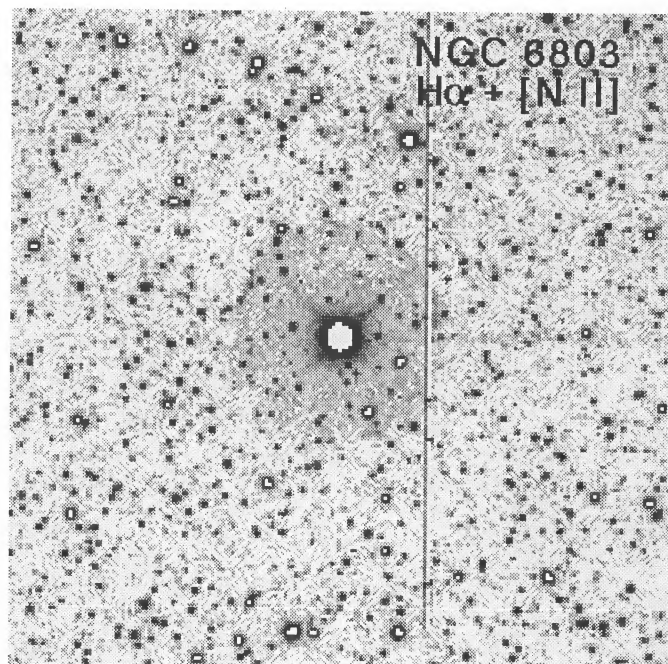


FIG. 6.—NGC 6803. See also the caption of Fig. 1. The field of view is 200 pixels.

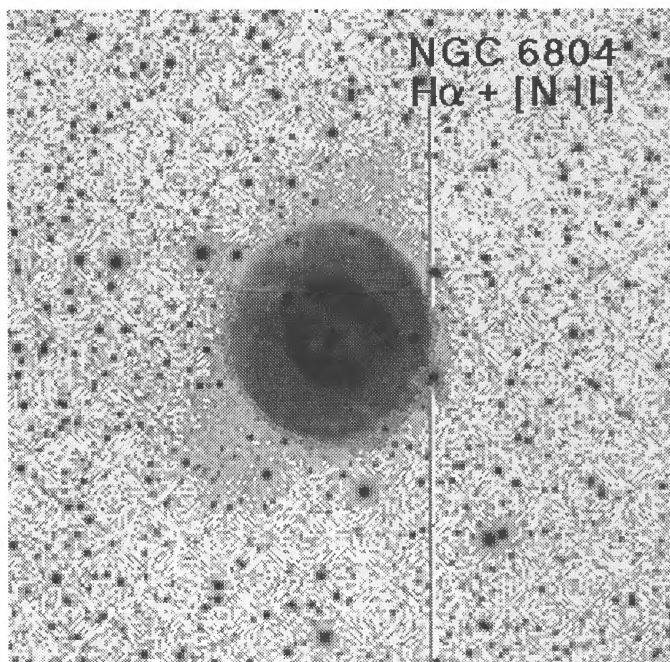


FIG. 7.—NGC 6804. See also the caption of Fig. 1. The field of view is 200 pixels.

The mottled appearance of the halo might be explained as a projection effect assuming that the halo is seen as a spherical bubble with a highly dimpled surface. The irregular outer edge of the halo observed in Figure 8 corroborates this suggestion.

Beyond the bright limb of the halo faint emission is seen. As discussed in Paper I, the faint outer emission is expected to arise in the same medium which confines the halo and causes its sharp leading edge to develop.

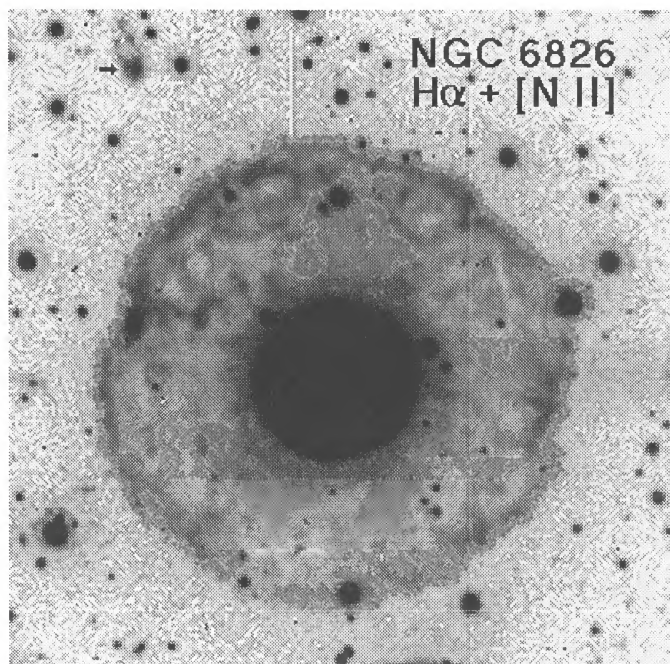


FIG. 8.—NGC 6826. See also the caption of Fig. 1. The field of view is 200 pixels.

At the E edge of the halo a bright knot is found at the location where the halo boundary is pinched (see Middlemass et al. 1991 for details). NE of the core by $108''$ is a small cometary nebula (marked by an arrow in Fig. 8) which points near the nucleus. These features are confirmed in the MRO observations. The comet is reminiscent of the features throughout the halo of NGC 6543.

NGC 6853 (PK 60–3°1; the “Dumbbell Nebula”).—The nebular and its halo overfill the field of view of the MRO and KPNO CCD. Consequently four 1000 s heavily overlapping images were made at MRO, aligned on field stars, and mosaicked to form the final image (Fig. 9, [Pl. 1]). Owing to time limitations only $H\alpha$ images were made of NGC 6853 and its halo. The image spans $900''$ in the E–W direction. Ted Gull (1990, private communication) confirms the existence of the halo from photographic observations. Millikan (1974) noted the existence of a halo of size $907''$ but did not publish a picture. Kwitter (1991, private communication) has made detailed observations of the halo of the Dumbbell in a variety of emission lines. The reader is referred to her future paper for details.

The halo is brightest to the north and fades in brightness azimuthally. Typical intensities are 2000 to 4000 times fainter than the brightest nebulosity. Except to the S, the halo appears to be mostly limb-brightened. A physical explanation for the N–S brightness asymmetry is not apparent. Perhaps the nebula moves northward through the ISM (Borkowski, Sarazin, & Soker 1990; Soker, Borkowski, & Sarazin 1991) so that the pressure exerted on the halo from this direction helps to confine and sharpen the leading edge on the northern side.

Radial “rays” of brightness connect the shell and the halo of the Dumbbell, much like faint radial rays seen in NGC 40. Two rays extend from bright jetlike features seen in the bright nebular interior (P.A. 30° and 150°). Other rays (some of which are decidedly nonradial) do not have conspicuous extensions into the nebular interior. Note that the extension of the bright ray in the SW part of the core (P.A. $\approx 240^\circ$) becomes dark in the halo, much like an ionization shadow. An IF can be seen at the end of the bright ray in the CCD images of B87.

The origin of the bright rays is unclear. If the halo is a partially ionized nebula, then the bright radial rays might be relatively highly ionized regions which are illuminated directly by stellar ionizing radiation seen through holes in an IF. However, no evidence of an IF at the base of the bright rays is obvious from the $H\alpha$, [O III], and [N II] filter CCD images presented by B87.

Note that hydrodynamic effects are not likely to lead to the development of radial features. An exception might be that if trapped high-pressure gas punctures the edge of the core then relatively dense, nebular gas can be entrained into the outward flow.

Molecular hydrogen has been mapped in the Dumbbell Nebula (Zuckerman & Gately 1989). Like the Ring, the brightest H_2 arises at the edge of the core. The H_2 is deeply embedded within the ionized halo.

NGC 6891 (PK 54–12°1).—Exposures taken at MRO through $H\alpha$ and [N II] filters of 300 seconds each were made only during our first run under highly variable sky conditions. The same faint halo seen by others (e.g., CJA) was detected in $H\alpha$. The halo is about 2500 times fainter than the nebula.

NGC 6894 (PK 69–2°1).—Like Abell 2 and IC 1454, the core and shell of this nebula are both round, and the core is only slightly smaller than the outer edge of the shell (B87;



FIG. 9.—Two representations of the same H α image of NGC 6853 taken at MRO. The intensities are displayed using two gray scales, one for the core and one for the exterior nebulosity. The logarithm of the intensities is displayed. The field of view is approximately 1000". The inset shows the structure in the white parts of the main figure.

BALICK, GONZALEZ, FRANK, & JACOBY (see 392, 588)

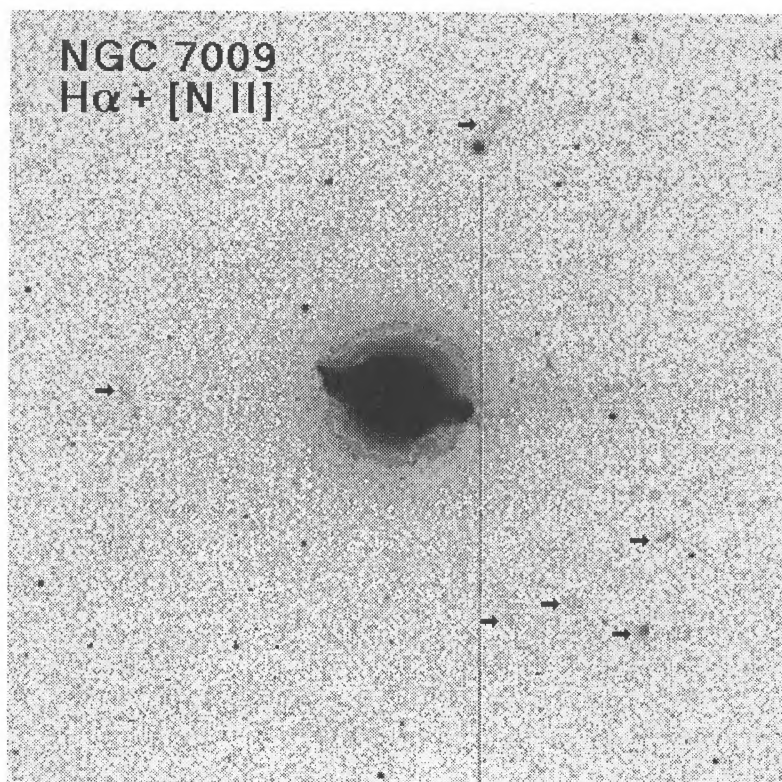


FIG. 10.—NGC 7009. See also the caption of Fig. 1. The field of view is 300 pixels

CJA). The MRO image reveals long, sinewy filaments throughout the 12' field of view of the CCD. However, no round, limb-brightened halo was detected at a level of 1/400 of the peak nebular brightness. Portions of the filaments proximate to the core of NGC 6894 were also seen by CJA. The filaments are brightest in the immediate vicinity of the nebula and fade with projected distance. Of the PN studied here, NGC 6894 has about the smallest Galactic latitude. Perhaps these bands are parts of the ambient disk ISM “illuminated” by stray UV photons from the nebula.

NGC 7009 (PK 37–34°1; the “Saturn Nebula”).—Like NGC 6543, the surface brightness of the core of NGC 7009 is very high. Also like NGC 6543, the Saturn Nebula has a morphology (e.g., ansae and “polar caps”) which differs somewhat from most of the other PN in the present survey. NGC 6543 has a very conspicuous halo, albeit irregular. Consequently a search for a halo in NGC 7009 was made as well.

KPNO observations (Fig. 10) shows no evidence of a halo like that surrounding NGC 6543. Scattered light within the telescope optics is seen as smooth emission in the immediate vicinity of the bright part of the nebula. However, several very faint nonstellar flocculi (indicated by arrows) lie between 1' and 1.5' E, SW and NW of the core. The flocculi are 10^4 times fainter than the core in this image. Since the core was heavily saturated the true brightness ratio is considerably higher. Consequently it is conceivable that the flocculi are telescope artifacts; nonetheless, images of bright stars made with the same system do not show such features.

Extensive observations of NGC 7009 were made at MRO. However, internal reflections in the telescope were found in all images. The telescope pointing was dithered (§ 2) and the brightest of the reflections were identified. However, fainter

ghosts and reflections may not have been removed. Consequently the MRO images neither confirm nor contradict the KPNO results.

NGC 7662 (PK 106–17°1).—The KPNO image of the halo of NGC 7662 filter is shown in Figure 11. It agrees nicely with that of Middlemass et al. (1991). POSS images inspected by Kaler (1974) show the same features. Deeper MRO images show that the halo is nearly circular, generally uniform in surface brightness, limb brightened, and fainter than the core by a factor of 20,000. Its radius is $\approx 72''$.

Fuzzy knots and small arcs are found in the SW and NW portions of the halo, especially along its leading edge. These knots are very highly ionized and hot (e.g., $[\text{O III}]/\text{H}\beta \approx 18$) and are discussed by Middlemass et al. (1991). Chu & Jacoby (1989) report that the $[\text{O III}]$ line width is 47 km s^{-1} throughout the halo. The halo expansion speed, Mach 2.5, is the largest of any PN in their survey.

An extremely unusual E–W jet can be seen 3' W of the nucleus in Figure 11. MRO observations confirm its reality. No counterpart to the E has been detected. Jetlike features in other PN are generally adjacent to the nebular core and deeply embedded within a halo (e.g., NGC 40, 6543, 7453). See Icke, Preston, & Balick (1989) for a discussion of jets in PN.

IC 1454 (PK 117+18°1).—The core-shell morphology of this object is strikingly similar to that of NGC 6894 and Abell 2, neither of which show halos. A halo is seen in the KPNO image (Fig. 12). The radius of the halo is $48''$ (to the steep outer intensity gradient), and its maximum surface brightness is 1%–2% of the core. Between the shell and the edge-brightened halo the surface brightness falls nearly to the noise limit. The outer regions of the halo of IC 1454 are more diffuse than the halos of most other PN studied here.

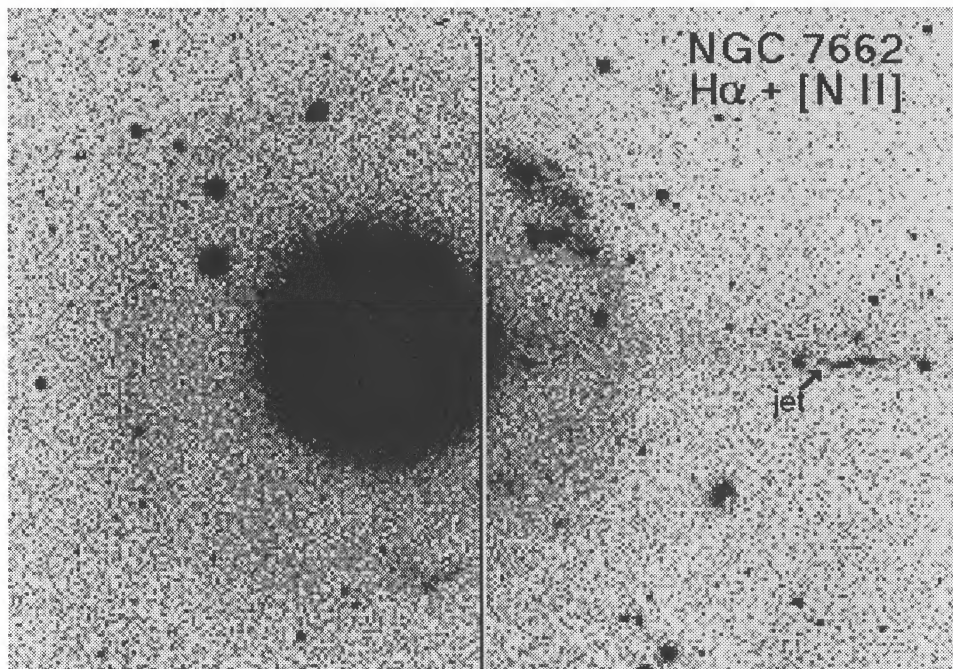


FIG. 11.—NGC 7662. See also the caption of Fig. 1. The field of view is 550×388 pixels

IC 3568 (PK 123 + 34° I).—IC 3568 is one of a small number of exceedingly round PN. Its morphology is classical: there is a very bright circular core of radius $4''$ surrounded by a conspicuous round shell whose brightness falls precipitously at a radius of $9''$ (see Paper I for a plot of the radial distribution of surface brightness). We expected to detect a halo owing to the morphological similarity between IC 3568 and many other PN with halos.

Faint emission is seen at radii as large as $18''$ in the KPNO image (Fig. 13). However, the surface brightness slowly declines to the noise level, and no evidence of a bright limb is observed to a limit of 10^{-4} of the nebular core. Consequently, apparent nebulosity beyond a radius of $9''$ is either evidence of scattered light in the telescope optics or a second and much fainter shell.

IC 4953 (PK 25 + 40° I).—The core of IC 4953 and NGC 6210 consist of very bright knots contained in a region about

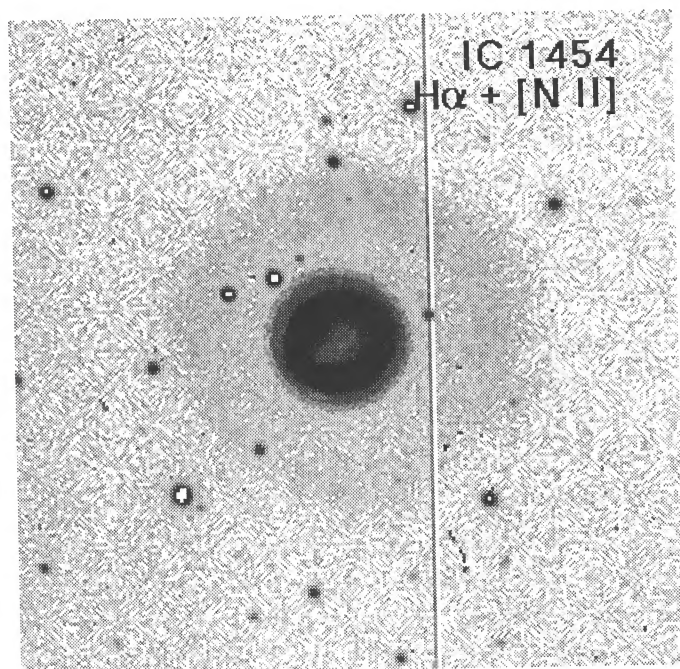


FIG. 12.—IC 1454. See also the caption of Fig. 1. The field of view is 200 pixels.

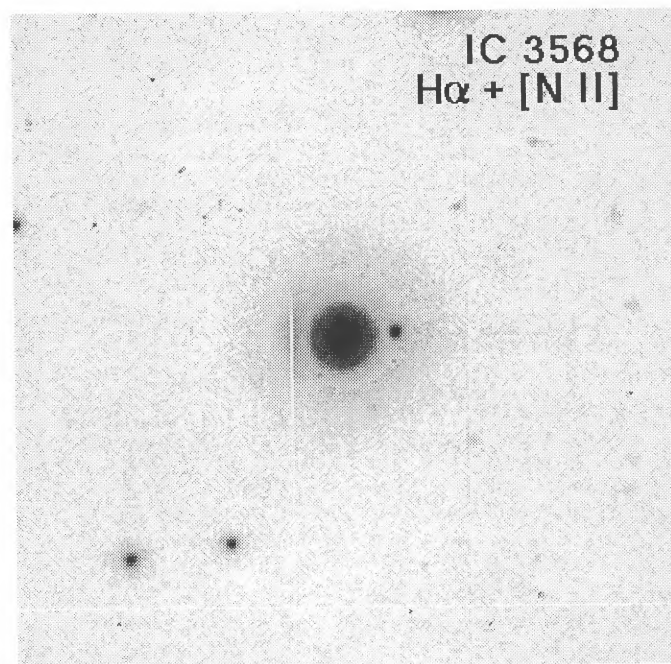


FIG. 13.—IC 3568. See also the caption of Fig. 1. The field of view is 200 pixels.

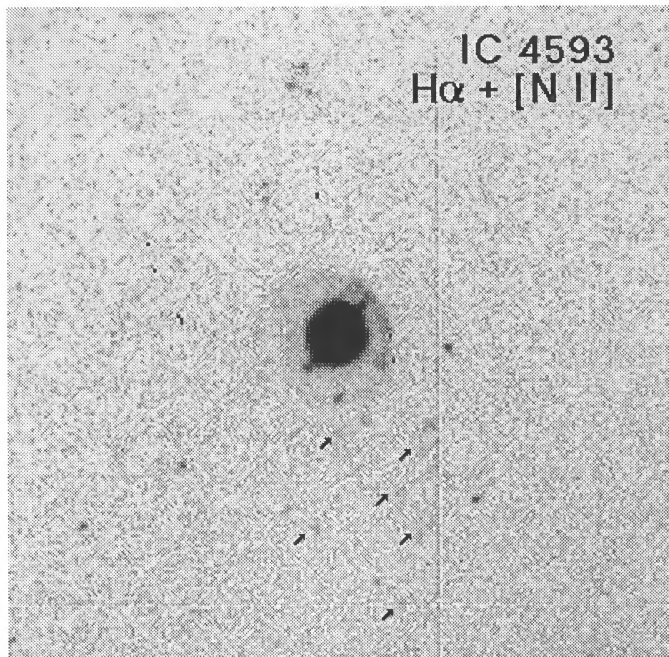


FIG. 14.—IC 4593. See also the caption of Fig. 1. The field of view is 200 pixels.

10" in diameter. In both cases jets or arms protrude from the clump of knots (as can be seen in Fig. 14 in position angle 130°). IC 4593 shows a faint halo whose shape is reminiscent of a bow shock. In this regard the outer halo of IC 4593 is very similar to that in the PN Abell 35 (Jacoby 1981). Such features are believed to be caused by motion of a PN and its halo through the interstellar medium (Borkowski, Sarazin, & Soker 1990; Soker, Borkowski, & Sarazin 1991).

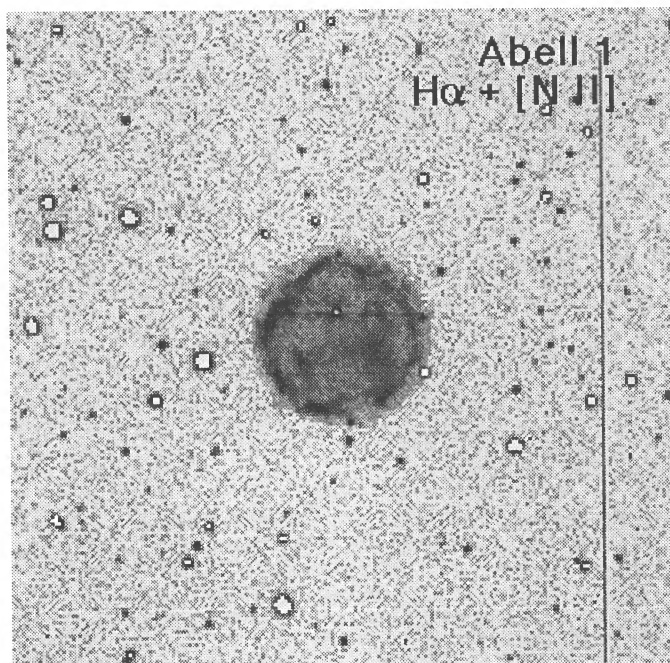


FIG. 15.—Abell 1. See also the caption of Fig. 1. The field of view is 200 pixels.

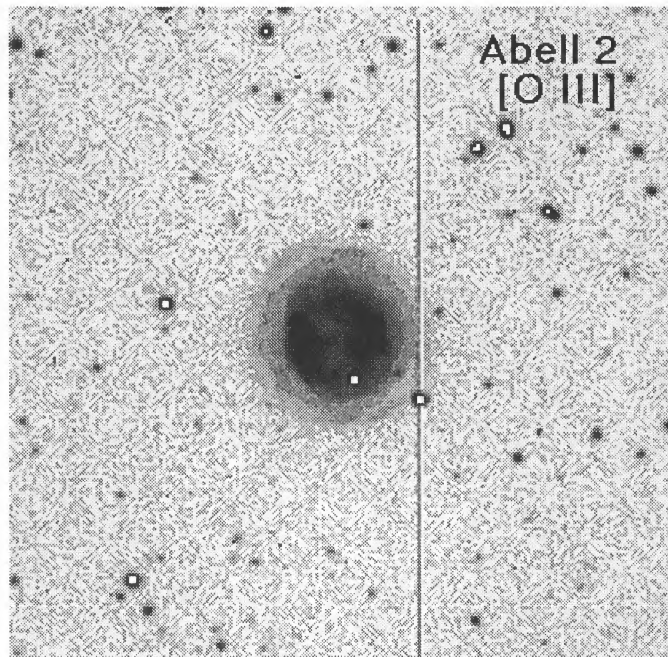


FIG. 16.—Abell 2. See also the caption of Fig. 1. The field of view is 200 pixels.

Various nonstellar knots are found S of the nebula. Some of these are marked by arrows in Figure 14. Their physical relationship to the core and envelope of IC 4593 is unclear.

Abell 1 (PK 119+6°1).—This is a round, limb-brightened nebula with no apparent interior core or shell (Fig. 15). The emission is clearly limb brightened, and the diameter is 25". Morphologically, the nebulosity can be considered to be dominated by a halo. The surface brightness of the halo, as estimated from the count rate per pixel, is characteristic of the more prominent halos found in many of the PN described above. Examples of other halo-dominated PNs include Abell 30, 39, and NGC 7139.

Abell 2 (PK 122-4°1).—Like NGC 6894 and IC 1454, the inner regions of Abell 2 (Fig. 16) consist of a round core surrounded by a thin shell (CJA). Indeed, the nebula is strikingly similar to NGC 2022. The shell is about an order of magnitude fainter than the core. No halo has been detected.

Abell 3 (PK 131+2°1).—The morphology of Abell 3 is similar to that of NGC 40: *to wit* a barrel-shaped core with fainter protrusions along its similar axis (Fig. 17). This type of structure is common amongst PN such as NGC 6905, 7048, and Abell 82. The major axis of Abell 3 is about 90", and its position angle is $\approx 50^\circ$. No halo is detected.

BD + 30°3639 (PK 64+5°1).—The surface brightness of the core of BD + 30°3639 is among the highest of all PN, and our deep images are badly saturated in the central regions. However, light is detected at large radii from the core in the KPNO image. One "shell" is found at a radius of 31" whose surface brightness is 4000 times less than that of the saturated peak of the core. At a radius of 82" is a much less obvious halo more than 50,000 times fainter than the core. There is a substantial possibility that both of these features are the artifacts caused by diffraction or scattering in the telescope as judged from the ghost images surrounding bright stars in other 4 m images. We consider the halo-like features described here to be of dubious reality. Confirming observations are difficult

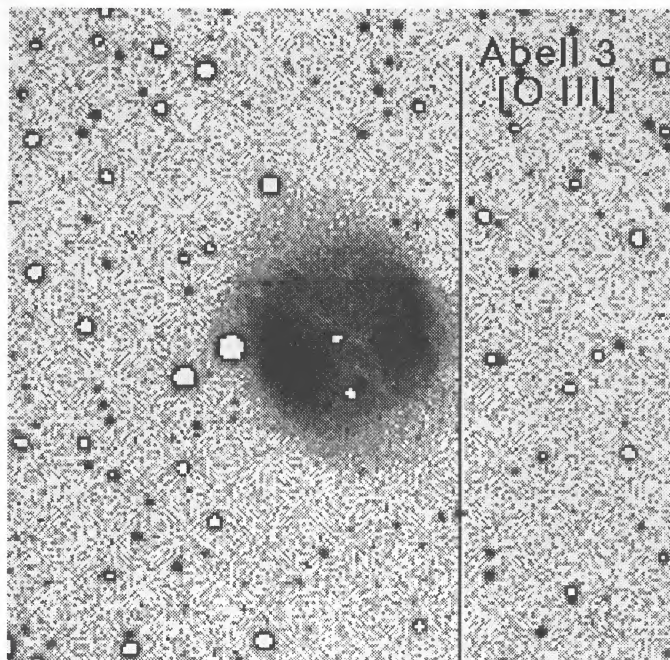


FIG. 17.—Abell 3. See also the caption of Fig. 1. The field of view is 200 pixels.

without a stellar coronagraph. No attempt to detect a halo was made at MRO.

4. GENERAL DISCUSSION OF HALOS

We address some of the features of halos found in the present sample. There are five issues:

1. Halo morphologies: the observed intensity distributions of halos (and shells) are remarkably uniform. What likely mechanism(s) can explain the morphologies of halos?

2. Halo ellipticities: the halos of PN are less elliptical than the shells and cores that they surround. What does this reveal of the symmetry of mass loss from the central star?

3. Halo confinement: limb brightening of halos suggests that they are pressure confined ($nT \approx 10^3 \text{ cm}^{-3} \text{ K}$). What is the source of confining material?

4. “The H_2 enigma”: the puzzling occurrence of H_2 emission from shells deep within the halos of NGC 6720 and 6853 forces a new look at nebular geometries and ionization histories. Can a reasonable model be proposed?

5. Constraints on mass loss: Do PN shell-halo geometries, kinematics, and abundance gradients provide directions for linking theories of mass ejection by deep thermal pulsations (e.g., Iben & Renzini 1983) to observables of PN?

4.1. Halo Morphologies

We begin by considering the thesis that halos evolve hydrodynamically rather than ballistically. To this end we consider the radial distribution of gas and compare the results to model computations of Paper I.

The average radial distributions of surface brightness were measured in concentric circular annuli drawn from the nuclei of those PN with halos. Figure 18 shows the azimuthally averaged radial surface brightness distribution of the halos of four PN measured after blanking the stars in the field. For NGC 6826, 7662, and IC 1454 the halo surface brightness falls

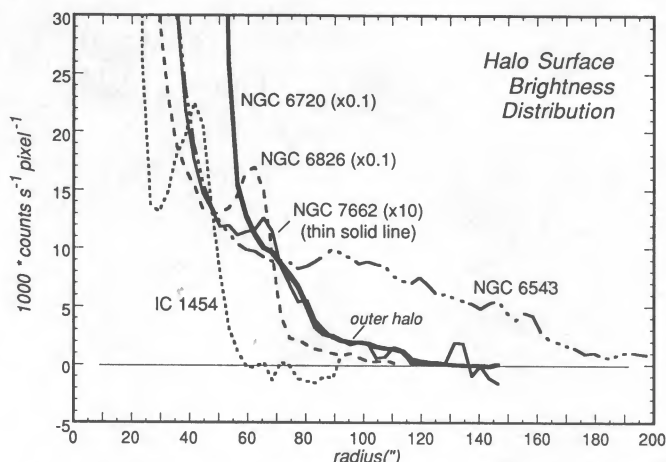


FIG. 18.—Azimuthally averaged radial distribution of surface brightness for the halos of NGC 6720, 6826, and 7662. Any ellipticity in the shape of the halos has been ignored. Intensities are in milliconcounts $\text{s}^{-1} \text{ pixel}^{-1}$ (mcps), where 1 cps corresponds to a surface brightness of $1.5 \times 10^{-15} \text{ ergs s}^{-1} \text{ cm}^{-2} \text{ arcsec}^{-2}$ in clear weather (see text). Halo radii are measured to the steepest part of the falling intensity gradient beyond the bright limb.

to a minimum and then rises abruptly at the outer edge. Qualitatively this behavior is in excellent agreement with the one-dimensional computational models of halos presented in Paper I.

The complexity (i.e., loops) within the relatively elliptical inner halo in NGC 6720 (see below) smears the radial intensity distribution. One’s visual impression is that both of its halos have much the same properties (i.e., limb-brightening) as circular ones.

Clearly the hydrodynamical evolution of pulses of stellar ejecta modeled in Paper I provides a natural framework for explaining the limb-brightened morphology of halos. Qualitatively, a pulse of material is ejected at $t = t_0$ and expands nearly ballistically at first. In the process its pressure drops as $(t - t_0)^2$. Eventually the outstreaming gas becomes partially confined by a medium upstream of roughly comparable pressure. (The source of the confining medium is discussed later.) Once this happens, gas flowing outward tends to pile up at the leading edge of the flow. Some of it also flows backward into the cavity created as the pulse expands. The natural result is a partially filled cavity, a slowly rising density distribution with radius, and a crisp forward edge.

A one-dimensional model for this process was computed in Paper I for reasonable but ad hoc initial and boundary conditions. (see their Fig. 10.) Their result is in excellent agreement with the observations.

The only other model, that of ballistic ejection and no confinement, cannot explain the most conspicuous character of the halos—their bright outer edges—without highly ad hoc assumptions about the time variability of mass ejection. For steady ejection the density will drop as r^{-2} , and the emission measure as r^{-3} . This is contrary to observations which show that the density increases with radius from the shell.

4.2. Halo Ellipticities

Next we consider the radii and ellipticities intrinsic to the leading edge of the cores, shells, and halos of the brighter PN in our sample. Bipolar PN are excluded. Operationally, we define the edge by a steep negative brightness gradient, that is,

TABLE 2
MAJOR AXIS RADIUS AND ELLIPTICITIES e OF PLANETARY NEBULA MORPHOLOGICAL COMPONENTS

NEBULA	CORE		SHELL		HALO		OUTER HALO	
	Radius	e	Radius	e	Radius	e	Radius	e
NGC 6720	42"	1.31	a	a	78"	1.15	115"	1.00
NGC 6826	9	2.0:	21"	1.68	68	1.03
NGC 6853	241	1.44	a	a	441:	1.10:
NGC 7662	8	1.50	16	1.22	72	1.05
IC 1454.....	14	1.05	19	1.02	48	1.02

^a We associate the inner structure with the core.

where isophotal contours are most crowded. The results are summarized in Table 2. In short, for any PN the more compact and bright the morphological component the greater its ratio of major to minor axis ratio e . Note that the largest halos are very nearly round in all cases. (NGC 6543's halo is too complex to estimate e).

Careful inspection of the images show that the major axes of all of the structural components are aligned. In other words, if each morphological component arises from outflows at different times, then memory of a preferred axis is retained in each outflow event.

The clear trend towards rounder outer structures begs for an explanation. Hydrodynamical effects will tend to spherize the mass distribution if the internal sound speed ($\approx 12 \text{ km s}^{-1}$) is comparable to the expansion speed of the halo. This may be important in the slowly expanding halos of NGC 2348, 6543, 6826, and 6891 (Chu & Jacoby 1989). Note also that if the halo expands into a medium of high ram pressure, the expansion velocity will drop quickly to the sound speed. No matter what its initial density distribution, a halo which expands at a constant velocity in all directions (e.g., adiabatically into a uniform medium) tends to become increasingly spherical as it grows. (This can also apply to the individual lobes of bipolars late in their evolution once the collimated wind abates.)

Also likely is that the earlier ejection pulses are more spherical than later ones. Pascoli (1990) has suggested that magnetic toroids which form deep within the star rise buoyantly to the photosphere and produce equatorially enhanced outflows at the surface. The higher surface gravity at later episodes will enhance the departures from isotropy. Morris (1987), Bond & Livio (1990), Soker & Livio (1989), Livio & Soker (1988), and others have suggested that nonisotropic outflows occur as the result of mass overflow in close binaries. As the stars approach one another the angular distribution of mass loss will become more collimated. Soker & Harpaz (1992) suggest that high-order nonradial oscillation modes dominate the mass ejection as the star's mass decreases. While no clear picture of the mass-loss process has yet emerged, all extant suggestions contain the kernels of explanations for the differing geometries of PN cores, shells, and halos.

No matter what mechanisms might affect the isotropy of stellar mass ejection, later pulses tend to overtake older ejecta and react hydrodynamically to the structure into which they flow. As all model computations show (e.g., Icke 1988), any pressure or density asymmetries already present from earlier episodes of ejecta tend to reshape the mass flow of the latest ejection and exaggerate the asymmetries that might have been present already. This alone argues that cores should be the most asymmetric of the nebular structural components.

In summary, there are a variety of plausible explanations for the roundness of halos. Consequently, little useful information about the history of mass ejection can be extracted from the geometries of halos.

4.3. Halo Confinement

The PN with known prominent halos surrounding their cores, and their Galactic latitudes are NGC 2438 (4°), 6543 (29°), 6720 (13°), 6826 (11°), 6853 (3°), 6891 (12°), 7662 (17°), IC 1298 (4°), 1454 (18°), and 4593 (40°). Limb-brightening is a common characteristic of all halos. Based on one-dimensional models in Paper I and others, the limb-brightening requires a confining medium with a pressure $nT \approx 10^3 \text{ cm}^{-3} \text{ K}$ at a halo radius $r_h \approx 0.5 \text{ pc}$ (i.e., a kinematic age of 10^4 yr). However, the high Galactic latitudes of the sample argue for confinement by gas in the Galaxy's lower halo or by a wind ejected even before the halo was expelled (a "red-giant wind").

Borkowski et al. (1990) and Soker et al. (1991) assume that confinement is provided by the ISM. This is necessary to explain the "head-tail" bowshock morphology of PN such as Abell 35 and NGC 246. The confining pressure P_g/k of the ISM and the lower regions of the Galactic halo is generally taken to be uniform and in the vicinity of $10^3 \text{ cm}^{-3} \text{ K}$, i.e., very close to the requisite pressure. For both reasons confinement by the ISM of the lower Galactic halo is a likely possibility in at least some cases. Indeed the ISM can be probed by measuring the ram pressure, i.e., the proper motion and expansion rate of the bowshock-type PN halos and shells.

Nonetheless the nucleus may be capable of providing its own confining medium. Assuming that a red giant wind (RGW) is characterized by a mass-loss rate of $\dot{M}_{\text{RGW}} \approx 10^{-7} M_\odot \text{ yr}^{-1}$ and a relative RGW-halo outflow velocity $u_{\text{RGW}} \approx 5 \text{ km s}^{-1}$, then the pressure P_{RGW}/k along the leading edge of the halo is $\dot{M}_{\text{RGW}} u_{\text{RGW}} (4\pi k r_h)^{-1}$ which is also close to $10^3 \text{ cm}^{-3} \text{ K}$. Hence either means of confinement, the ISM or a previous RGW, provides the requisite ram pressure to form a limb-brightened halo.

Can observations determine the nature of the confining medium? Of course, the ram pressure of the halo decreases as it expands (as t^{-1}). On the one hand, the forward pressure provided by the pressure of the ISM remains constant. Hence the expansion speed of the halo is expected to drop quickly for ISM confinement. On the other hand, the RGW expands and its pressure drops at a rate which depends on its expansion speed. If the RGW and halo expansion speeds are the same, then the decreasing pressure of the halo is matched by the decreasing forward pressure of the RGW. In this case the halo changes only in its scale but not its shape or velocity (to first order). The kinematic data of Chu & Jacoby (1989) argue that

most PN halos expand sonically or subsonically. This might be interpreted as favoring confinement by the ISM.

One final note on the sharp edges. Conceivably they are simply the result of an IF rather than the ram pressure of a confining medium. Such an IF should be most visible in the lines of low-ionization species such as N^+ . [N II] images taken at MRO fail to show evidence of an IF. Accordingly, we dismiss this hypothesis.

However, ionization effects might be important in other ways. Consider a recombining halo with a radially decreasing density distribution. Recombination and cooling times are inversely proportional to the free electron density. Therefore the inner, densest regions are the first to cool and recombine. It follows that the inner parts of the halo may be faintest only because these regions are less ionized. This should be especially true for temperature sensitive forbidden lines. Ratios of images in [O III] and [N II] can test this explanation because singly ionized species have significantly longer recombination times than doubly ionized species.

4.4. The H_2 Enigma

The famous ring-shaped nebular core of NGC 6720 is bright in H I recombination and [O III] lines. CCD images of the core in [N II] and [O I] (e.g., B87) are strongly limb brightened and suggest that an ionization front (IF) surrounds this core. To reinforce this hypothesis, the collisionally excited H_2 appears to be virtually coincident with the [O I], as might be expected since both species must lie in a warm, largely neutral region where the transitions' upper levels can be excited by thermal collisions of several eV. This is the classical picture of an ionization-bounded nebula in which no ionizing photons produced by the star can escape from the core.

The puzzle is that the core and the H_2 emission region are both found to lie *inside* of (two) ionized halos. In this section we explore models for the nebulae that might resolve this dilemma.

Before opening this discussion we comment on the superficially similar situation in the Dumbbell Nebula. The geometry of NGC 6583 is roughly similar to that of the Ring Nebula, except that there is no indication of any IF associated with the nebular core. Also, the H_2 has not been mapped with sufficient angular resolution to establish its location relative to the halo with much certainty (Zuckerman & Gatley 1988). Consequently the present discussion focuses primarily on the better studied case of the NGC 6720.

To structure the discussion we begin with a simple but obviously incorrect "baseline" model. The core and halos of NGC 6720 are assumed to be spherically symmetric and concentric. Each component is in ionization and statistical equilibrium, and each has constant mass. The nebula expands homogeneously and slowly. We further assume that an IF within the core is opaque to ionizing radiation. Thus any gas outside of the core is shielded from ionizing photons from the nucleus of NGC 6720.

We consider three variations of the baseline model:

"*Inclined Bipolar*".—Rather than being spherical, the nebula is assumed to be bipolar much like NGC 2346. To explain its ringlike shape we assume that the nebula's symmetry axis is highly inclined. The [O I] and H_2 emission seen at the edge of the core actually arises in a belt surrounding the "waist" of the nebula. The large halo is interpreted as the two

large bipolar lobes of the nebula seen in projection outside the waist.

"*Porous IF Bubble*".—Numerous and unresolved holes in the spherical IF permit some ionizing photons to penetrate through the molecular and neutral IF into the nebula's halo.

"*Recent Bubble Ejection*".—The halos of NGC 6720 were once ionized by the central star. However, gas recently ejected by the star forms a new core (now the Ring) in which the IF and a molecular medium are temporarily trapped. Today the halo consists of a partially ionized gas in the process of recombining. See Breitschwerdt & Kahn (1990) for a discussion of the evolving nebular ionization.

We now subject these models to closer scrutiny and consider future experimental tests which might be able to test their validity.

"*Inclined Bipolar*".—Let us first consider some of the observed properties of NGC 2346. Zuckerman & Gatley (1988) and Webster et al. (1988) found the molecular hydrogen to lie along the perimeter of the hourglass-shaped nebula. B87 finds much the same distribution of [N II] and [O I]. All of these lines are especially bright at the waist. Were NGC 2346 to be viewed nearly pole-on a bright, thin ring of [N II], [O I], and H_2 would appear to be nearly coincident with a bright ring of [O III] emission at the nebula's waist. The ring would appear to be embedded within a halo of faint, extended $H\alpha$, [O III], and [N II] emission formed by the large, faint bipolar lobes projected on the sky.

Is NGC 6720 a bipolar observed pole-on? Perhaps the easiest test is to carefully map its kinematics. Again referring to NGC 2346, the kinematics in $H\alpha$ and [N II] observed by Icke et al. (1989) show a very pronounced pattern of lobe expansion characterized by expansion velocities of $\pm 80 \text{ km s}^{-1}$ and much smaller velocities near the waist. By analogy, the expansion velocities in the faint halos of NGC 6720 should be similar. Chu & Jacoby (1989), who observed the nebula only in one position angle, find opposite trends: the expansion speed of [N II] lines from the core (i.e., waist) is 42 km s^{-1} whereas that of the halo (i.e., lobes) is 18 km s^{-1} .

There are two additional problems with this strictly geometric model. Firstly, unless we view the nebula exactly along its symmetry axis, the overlapping, nonconcentric lobes of NGC 6720 that form the halo in projection on the sky should *increase* the apparent major-to-minor axis ratio of the halo relative to that of the core. The opposite is observed: the halo is less elliptical than the waist that forms the central bright ring. Secondly, this model does not naturally account for the two concentric halos in NGC 6720 reported here. Hence we consider the model of a tilted bipolar as untenable.

"*Porous IF Bubble*".—Stellar UV radiation escapes through numerous unidentifiable holes in the IF of the core (which we view as the ring) and ionizes gas in the two halos. Since the halo is slow wind ejected much earlier the expansion speed of the halo should be relatively slow: 18 km s^{-1} is a somewhat large but acceptable value. The core would be expanding faster, though 42 km s^{-1} seems a bit excessive compared to the cores of most other PN (Icke et al. 1989, and references therein). The model can be tested by more extensive kinematic observations of the halo.

A potential problem with this model is its longevity. Photon-heated gas evaporates from the cold, neutral parts of the bubble-shaped core into its interior cavity. Eventually the core and any molecular regions embedded within it are dissolved. (The time scale is difficult to compute without knowledge of

the core density distribution and mass.) If the interior of the core is hot, then heat can be conducted into the core which, in turn accelerates the evaporation process.

Recent Bubble Ejection.—This is a variation of the last model which drops the assumption of constant mass. Prior to the last mass ejection the nebula consisted of only the same two nested and ionized halos seen today. Then a pulse of mass loss occurred. The atmosphere of the star was too cool ($\leq 20,000$ K) to destroy all of the molecules during the latest cycle of ejection. The latest pulse with some of its molecules intact has expanded to become the core, or ring, of the nebula.

At the present time stellar ionizing radiation is still absorbed in the new core. The molecular gas in the core is shielded from direct stellar photons which can dissociate the H_2 (This will change as the core expands.) As for the halo, it is now cut off from ionizing radiation from the star. Gas in the halo is in the process of recombining with a characteristic time scale of $10^5(n_e)^{-1}$ yr $\approx 10,000$ yr or more, where n_e is the electron density. Hence the halo is partially ionized. Radial rays occur where stellar radiation leaks through the IF

Like the porous bubble model, the halo is expected to be only slowly expanding, as observed. A necessary condition for this model is that the expansion age of the core, T_c , is considerably less than that of the halo, T_h . The relative ages of core and halo are given by the ratios of their respective angular diameters divided by their expansion speeds. Using the data of Table 2 and the Chu & Jacoby (1989) observations we derive $T_c/T_h \approx 0.2$, a very comfortable result.

Of the three models considered here, the model of recent bubble ejection seems most in accord with extant observational data.

4.5. Constraints on Mass Loss

The nested halo-shell structures examined in this paper suggested multiple mass-loss events by the central star. What drives these mass-loss events? Numerical simulations (Tuchman & Barkat 1980) have demonstrated that enhanced mass loss may be initiated by the thermal pulses of the AGB progenitor. If this does in fact occur then it is natural to associate a thermal-pulse-driven event with the superwind (e.g., Iben & Renzini 1983). Since a helium-burning star will experience a number of thermal flashes it follows that there will be a number of superwind events and, hence, nested structures within the nebula.

The thermal pulse-superwind connection can be investigated using the properties of shells and halos of PN. Iben & Renzini (1983) derived theoretical relationships between the core mass of an AGB star and the interpulse time. The halo and shell times expansion times can be found from measurements of halo radii (which requires knowledge of the PN distance) and expansion velocities. This interpulse time can be used to determine the mass of the nucleus' progenitor. These ideas will be pursued in future observations.

5. SUMMARY

The detection of faint, large, round, ionized, limb-brightened halos of emission surrounding several PN is reported. Some halos are more than 10^4 times fainter than the bright, smaller cores with which they are associated. Their appearance is not systematic for other morphological classes; i.e., some PN with virtually identical structures will show halos, whereas others do not. Other PN halos associated with bipolar PN are found.

Spectroscopic data analyzed by Middlemass et al. (1991) and references within show that the masses of halos are comparable to the masses of PN cores, so masses of PN and their rate of mass return to the ISM may have been systematically underestimated.

Halos are being detected in increasing numbers of PN as observational sensitivity increases, so it is easy to conjecture that halos are a common characteristic of many PN. However, the detection of additional halos is going to be difficult. The detection rate is presently limited by the dynamic range of telescope imaging (i.e., false halos caused by small-scale imperfections in the optics and internal reflections within the camera or focal reducers) as well as sensitivity. Coronagraphic techniques should be used for deeper detection surveys.

Halos, as a class, are remarkably uniform in their morphologies. This argues for a common evolutionary history for all halos. We concur with the suggestion that halos are the remnants of older pulses of mass ejected from the central star. This picture is nicely consistent with all present observations provided that the evolution of the halos is essentially a hydrodynamical process. In particular, the radial brightness distribution of halos is easily explained if a confining medium of pressure $nT \approx 10^3$ cm $^{-3}$ K is present.

Curiously, the molecular regions of NGC 6720 and 6853 are embedded within the ionized halos that surround them. A possible explanation is that the molecule-rich core, ejected only recently, is expanding into a recombining and partially ionized halo. However, other explanations are also potentially viable.

The double halo of NGC 6720 and the presence of molecular emission within the halos are both surprises. We might end this paper on a sobering note by remarking that NGC 6720 is often considered the prototype planetary nebula. If this is true, then we have only begun to understand the morphologies and evolutionary history of all PN.

It is a pleasure to acknowledge the crucial help and helpful advice of Patrick Waddell in making the observations at MRO. We also wish to thank Dave Chamberlin who observed IC 4593 for us. A. F. wishes to gratefully acknowledge his discussion with Wil van der Veen concerning the thermal pulse-superwind connection. We are very grateful to the Ford Aerospace Corp. for the loan of their excellent CCD to MRO. This research was sponsored by NSF grant AST 89-13639. Astronomical image processing at the University of Washington was established by NSF grant AST 83-10552.

REFERENCES

- Balick, B. 1987, *AJ*, 94, 671 (B87)
 Bond, H. E., & Livio, M. 1990, *ApJ*, 355, 568
 Borkowski, K. J., Sarazin, C. L., & Soker, N. 1990, *ApJ*, 360, 173
 Breitschwerdt, D., & Kahn, F. D. 1990, *MNRAS*, 244, 521
 Chu, Y.-H., & Jacoby, G. H. 1989, In *IAU Symp.* 131, Planetary Nebulae, ed. S. Torres-Peimbert (Dordrecht: Kluwer), 198
 Chu, Y.-H., Jacoby, G. H., & Arendt, R. 1987, *ApJS*, 64, 529 (CJA)
 Dyson, J. E., & Hartquist, T. W. 1992, *Astrophys. Lett.*, in press
 Frank, A., Balick, B., & Riley, J. 1990, *AJ*, 100, 1903 (Paper I)
 Greenhouse, M. A., Hayward, T. L., & Thronson, H. A., Jr. 1988, *ApJ*, 325, 604
 Iben, I., & Renzini, A. 1983, *ARA&A*, 21, 271
 Icke, V. 1988, *A&A*, 202, 177
 Icke, V., Preston, H. L., & Balick, B. 1989, *AJ*, 97, 462
 Jacoby, G. H. 1981, *ApJ*, 244, 903
 Jewitt, D. C., Danielson, E. G., & Kupferman, P. N. 1986, *ApJ*, 302, 727
 Kaler, J. B. 1974, *AJ*, 79, 594
 Livio, M., & Soker, N. 1988, *ApJ*, 329, 764
 Louise, R. 1974, *A&A*, 34, 21
 ———. 1981, *A&A*, 102, 303
 Marten, H., & Schönberner, D. 1992, *A&A*, 248, 590
 Meaburn, J., Nicholson, R., Bryce, M., Dyson, J. E., & Walsh, J. R. 1992, *MNRAS*, in press

- Middlemass, D., Clegg, R. E. S., Walsh, J. R., & Harrington, J. P. 1991, MNRAS, 251, 284
Millikan, A. G. 1974, AJ, 79, 1259
Moreno, M. A., & López, J. A. 1987, A&A, 178, 319
Morris, M. 1987, PASP, 99, 1115
Pascoli, G. 1990, From Miras to Planetary Nebulae: Which Path for Stellar Evolution? ed. M. O. Mennessier & A. Omont (Gif-sur-Yvette: Éditions Frontières), 90
Plait, P., & Soker, N. 1983, ApJ, 99, 1881
Schönberner, D. 1983, ApJ, 272, 708
Soker, N., Borkowski, K. J., & Sarazin, C. L. 1991, AJ, 102, 1381
Soker, N., & Harpaz, A. 1992, ApJ, submitted
Soker, N., & Livio, M. 1989, ApJ, 339, 268
Tuchman, Y., & Barkat, Z. 1989, ApJ, 294, 199
Webster, B. L., Payne, P. W., Storey, J. W. V., & Dopita, M. A. 1988, MNRAS, 235, 533
Zuckerman, B., & Gatley, I. 1988, ApJ, 324, 501